

Analysis of Direct Liquid-Solid Contact Heat Transfer in Monodispersed Spray Cooling

Brian Delcorio* and Kyung-Jin Choi†

University of Illinois at Chicago, Chicago, Illinois 60680

The heat-transfer characteristics of a single droplet and spray impacting upon a horizontal surface heated above the Leidenfrost temperature are analytically investigated. The heat-transfer model of a single impacting droplet is developed, based on the postulate that heat transfer through direct contact is the dominant mechanism of the droplet impacting heat transfer. Heat-transfer models of spray are also developed by expanding the single droplet model to include the effects of droplet interference upon the impacting dynamics. A criterion value of liquid mass flux for classifying a spray as "sparse" or "dense" is established. The analytical models are compared with the existing experimental results, and they are found to be in good agreement.

Nomenclature

$A_s(t)$	= instantaneous droplet spreading area [mm ²]
A_i	= heating target area [cm ²]
c_p	= specific heat [J/kg K]
D_d	= droplet diameter [mm]
$D_s(t)$	= instantaneous droplet spreading diameter [mm]
H	= distance between a nozzle and hot surface [cm]
h_{fg}	= latent heat of vaporization [J/kg]
i	= reduction rate of spreading area
k	= thermal conductivity [W/m K]
L	= dimension of square matrix [cm]
m_d	= mass of a droplet [g]
m''	= mass flux of spray [g/cm ² s]
N	= number of droplets in a square plane
Q	= total heat transferred to a spray [J]
q	= total heat energy transferred to a droplet [J]
$\dot{q}(t)$	= instantaneous heat transfer rate per droplet [W]
$q''(t)$	= instantaneous heat flux [W/m ²]
R_{sp}	= radius of conical spray pattern on the hot surface [cm]
r_c	= radius of idealized surface cavity [mm]
T	= temperature [K]
ΔT_{sub}	= subcooling temperature, $T_{sat} - T_{i,0}$ [K]
t	= time [s]
t_c	= direct contact time [s]
U_d	= Droplet impaction velocity [m/s]
We	= Weber member, $D_d U_d / \sigma$
x	= distance upward from hot surface [mm]

Subscripts

ct	= critical
i	= at the liquid-solid interface
ℓ	= liquid
max	= maximum
o	= initial
s	= solid
sat	= at saturation condition
t	= at transitional condition
v	= vapor
α	= thermal diffusivity [m ² /s]

ϵ	= heat transfer effectiveness defined in Eqs. (15–17)
ρ	= density [kg/m ³]
σ	= surface tension [N/m]

Introduction

THE process of cooling a high temperature surface with a spray is currently used in various industries, and promises to be beneficial to many new and emerging technologies. Spray cooling is attractive for use in these areas since spray cooling provides for both the effective use of the coolant and the high density of heat dissipation, required by these technologies. In general, the effectiveness associated with spray cooling is higher than other cooling processes mainly due to the fact that the contact surface area between the liquid and the hot surface is increased with the spray process.

Previous investigations related to impacting spray heat transfer have concentrated on impaction of either a single isolated droplet, a commercial spray, or a monodispersed spray. A monodispersed spray is defined in this study as a spray of uniform sized droplets, in which droplets are uniformly distributed, while a commercial spray refers to a spray produced by a commercial nozzle. Sprays produced by commercial nozzles are usually dense and consist of droplets with a spectrum of diameters and velocities.

There have been several studies^{1–8} on a single droplet impaction on surfaces at temperatures above the Leidenfrost temperature. These studies have yielded much valuable information on vapor film development beneath the droplet, effect of droplet subcooling on heat transfer, and droplet impaction dynamics. The information provided by the isolated droplet studies are essential in the understanding of the heat-transfer mechanism of an impinging spray. However, this information is not directly applicable to a dense spray due to the effect of droplet interaction on the heated surface. There also have been a number of studies on the heat-transfer characteristics of a dense spray upon hot surfaces.^{9–13} The droplet interactions, however, become complicated by the broad spectrum of drop diameter and velocity that make up the commercial spray. As a result, evolution of individual spreading dynamics is interfered with, hence, masking the effects of spray parameters such as drop initial diameter and initial velocity. Although these studies provided useful information on total heat-transfer rates, they did not give much insight into the effects of spray parameters on the heat-transfer rate. In a third type of spray, cooling heat transfer, monodispersed sprays were used for observing effects of droplet interactions on heat transfer.^{14,22} This type of study, where spray parameters were controllable has provided some insight into mech-

Received April 19, 1990; revision received Oct. 22, 1990; accepted for publication Nov. 2, 1990. Copyright © 1991 by the American Institute of Aeronautics and Astronautics, Inc. All rights reserved.

*Research Assistant, Mechanical Engineering Department; currently, Commonwealth Edison Co., Chicago, IL.

†Assistant Professor, Mechanical Engineering Department. Member AIAA.

anism of heat transfer and effects of the drop size, mass flow rate, and impacting velocity on heat transfer. Even though some information concerning effect of spray parameters has been acquired, much uncertainty still exists. Further investigation of heat-transfer mechanisms involved in monodispersed sprays is needed.

The mechanism by which of heat transfer during droplet impaction upon a surface at a temperature above the Leidenfrost temperature has been studied before, but there has been disagreement over the heat-transfer mechanism. Previous heat-transfer modeling of impacting droplets can be classified into groups based on the dominant mode of heat transfer. A number of researchers modeled the droplet-wall heat transfer based on the postulate that a vapor layer forms instantaneously beneath the droplet, obstructing direct contact between the spreading liquid drop and the hot surface.^{1,3,4} The heat-transfer model was developed based on the conduction process through a well-developed vapor film. As a result, vapor-film conduction models predict much smaller heat transfer than that found experimentally by Pederson² and Kendall and Rohsenow.³ This discrepancy was explained by introducing gas convection which might take place during a droplet impacting process.³ This postulate was extended even to the case of spray heat transfer by some investigators.^{10,12} They suggested that air convection induced by droplet movement is the dominant mechanism of droplet impacting heat transfer. In contrast, some researchers suggested that a vapor film does not develop instantaneously, but after a period of direct contact between the liquid droplet and the solid surface.^{6,11,13} These investigators believed that heat conduction through a liquid-solid direct contact takes place until a fully developed vapor film establishes beneath the liquid droplet. Recently, Inada et al.⁷ measured optically the vapor development and thickness. They observed that a significant vapor film is present only for the latter half of the droplet's residence time upon the hot surface. In addition, the experimental results by Choi and Yao¹⁴ for monodispersed spray cooling heat transfer showed that the liquid-wall direct contact heat transfer was a dominant mode in the cooling process, while air convection had little to do with overall heat-transfer performance.

The present authors suggest that the direct liquid-solid contact heat transfer is the dominating mechanism of heat transfer in impacting single droplet or spray on a hot surface. Therefore, the objective of this study is to develop analytical models of impacting droplets on the hypothesis that only direct liquid-solid contact heat transfer is significant. Through analytical modeling, heat transfer for impacting single droplet of various diameters, impacting velocities, and subcooling is predicted. The model for single droplet impaction is extended to predict the heat-transfer characteristics of monodispersed sprays, by considering the effects of droplet interference on the spreading dynamics during an impacting process.

Analytical Models

Single Droplet Impacting Heat Transfer

Phase-Change Delay Time

The interaction between a normally impacting single droplet and a hot surface above the Leidenfrost temperature can be characterized as a two-step process. Interaction consists of a period of direct liquid-solid contact followed by a period in which a vapor film develops beneath the droplet. Direct liquid-solid contact between a liquid droplet and a hot surface can be attributed to a certain finite time required for phase change to occur at the bottom of the droplet. The phase change occurs by means of homogeneous nucleate boiling at the liquid-solid interface. This phenomenon in single droplet impaction has been experimentally observed in the works of Wachters and Westerling,¹ Pederson,² Takeuchi et al.,⁵ and

Inada et al.⁸ Using high speed photography, nuclei of trapped vapor were observed to grow from the hot surface. Through nucleate boiling, a well-developed vapor film is later produced. Even though some investigators assumed that the direct contact time is very short and heat transfer during this time period can be neglected, it is the opinion of the present authors that direct contact heat transfer is significant in the droplet impacting heat-transfer process.

Based on this postulate, the liquid-solid direct contact time and the total heat transfer rate by conduction were calculated. In the analysis of direct contact time, liquid internal motion inside a droplet was neglected for simplification, and a model of subcooled pool boiling was employed. For nucleate boiling to initiate, the presence of trapped vapor in cavities on the surface is necessary. This situation is schematically depicted in Fig. 1, which shows a conical cavity on the surface with a hemispherical vapor nucleus sitting at the cavity opening. The liquid temperature far away from the wall is $T_{l,0}$ and the solid surface temperature is T_s . Hsu¹⁵ postulated that the criterion for the onset of nucleate boiling (ONB) from a cavity is that the lowest temperature on the vapor nucleus surface should be greater than the temperature to maintain a state of thermodynamic equilibrium. As long as the condition of thermodynamic equilibrium is satisfied the vapor nucleus experiences little growth. When considering ONB, only the time required to reach a nonequilibrium state is significant. This time is frequently called the waiting time and is discussed further by Han and Griffith.¹⁶ From the equation of static equilibrium for a vapor nucleus in a cavity of radius r_c , the maximum vapor temperature for which the thermodynamic equilibrium is maintained is given by Hsu¹⁵ as

$$T_v = \frac{R T_{sat} T_v}{h_{fg} M} \frac{(1 + \xi)}{1} + T_{sat} \quad (1)$$

where $\xi = 2\sigma/P_v r_c$, R = gas constant of water vapor, M = molecular weight of water vapor

The liquid temperature distribution in the vicinity of the hot surface was obtained by Han and Griffith¹⁶ by treating the liquid layer as a solid slab. However, obtaining the liquid temperature distribution for the case of an impacting isolated droplet is much more complicated since it involves boiling heat transfer coupled with the dynamics of impaction. Boiling heat transfer under simpler conditions is not completely understood, and when the additional complication of impaction dynamics is added, the problem becomes very complicated. Therefore, to simplify this problem, a similar approach to that taken by Han and Griffith¹⁶ for subcooled nucleate boiling is applied in the present study to an impacting droplet. The interaction between a droplet and a hot surface is assumed to be an interaction between two semi-infinite solid slabs, i.e., one for the liquid and one for the metal substrate. Previously, several investigators^{6,11,13} have also applied this assumption in their analyses of impacting droplet heat transfer. The resulting transient temperature profile is then given by Carslaw and Jaeger¹⁸ as

$$T_l(x, t) = T_{l,0} + \frac{T_{l,0} - T_{s,0}}{1 + c} \left[\operatorname{erf} \frac{x}{2\sqrt{\alpha_l t}} - 1 \right] \quad (2)$$

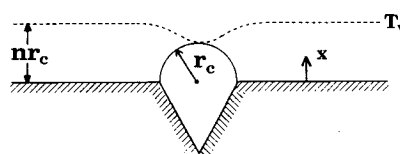


Fig. 1 Schematic of bubble formation in a cavity.

where $T_{\ell,0}$, $T_{s,0}$ and erf are initial liquid and solid temperatures and error function, respectively, and c is defined as

$$c = \frac{k_\ell \alpha_\ell^{-1/2}}{k_s \alpha_s^{-1/2}}$$

Therefore, as mentioned before, when the liquid temperature at the distance of an isothermal line passing through the top point of the vapor nucleus of Fig. 1 (i.e., the lowest temperature on the vapor nucleus surface) is higher than the equilibrium temperature T_v , the thermostatic equilibrium breaks down, and, in turn, ONB occurs. The distance of the isotherm from the hot surface, nr_c , was determined by Han and Griffith¹⁶ as $1.5 r_c$, but Hsu¹⁵ suggested a value of $2.0 r_c$. In this study, $2.0 r_c$ is applied. The phase-change delay time, t_c , also depends upon the cavity radius, r_c . On any surface a range of cavity sizes exists, but not all the cavities are active nucleation sites. The most favorable cavity size was studied in detail by Han and Griffith.¹⁶ For water on a smooth metallic surface the maximum cavity size was measured by Brown¹⁷ to be about $5 \mu\text{m}$ in radius. This value of cavity size is used in the present analysis. Then, the time required for the onset of nucleate boiling can be determined from Eqs. (1) and (2). This is the time needed for the liquid temperature at a distance of $2.0 r_c$ (i.e., $x = 10 \mu\text{m}$) to be heated to the equilibrium temperature, T_v . When the criterion is met, nucleation proceeds and a well-developed vapor film is formed beneath the droplet, obstructing direct contact between the liquid and solid. Then, the resulting direct contact duration is given as

$$t_c = \frac{r_c^2}{\alpha_\ell} \left[\text{erfc}^{-1} \left(\frac{(T_v - T_{\ell,0})(1 + c)}{(T_{s,0} - T_{\ell,0})} \right) \right]^{-2} \quad (3)$$

where erfc^{-1} is an inverse of complementary error function.

Direct Liquid-Solid Contact Heat Transfer

Calculation of heat transfer rate during droplet impaction is performed with the following assumptions:

- 1) During the direct liquid-solid contact time, the liquid becomes superheated and heat transfer from the solid to the liquid occurs only through conduction.
- 2) After vapor-film formation beneath the liquid droplet, the heat-transfer rate by conduction through the vapor film is neglected.
- 3) No contact resistance between the solid surface and the liquid film exists.
- 4) One-dimensional transient heat conduction takes place during the direct contact period.
- 5) The interface temperature between the solid and liquid does not change with time during the direct contact period.

When a hot surface assumed as a semi-infinite body is placed in contact with a cold liquid, the heat flux at the interface is then calculated from Ref. 18

$$q''_{s,i}(t) = k_s \frac{T_{s,0} - T_i}{\sqrt{\pi \alpha_s t}} \quad (4)$$

where T_i is the solid-liquid interface temperature. The interface temperature T_i can be calculated at $x = 0$ in Eq. (2). However, the actual interface temperature would be lower than this calculated value due to the effects of liquid internal motion and the partial vaporization of liquid during the conduction process. The instantaneous heat-transfer rate from the solid to liquid is

$$\dot{q}(t) = q''_{s,i}(t) A_s(t) \quad (5)$$

The transient spreading area of the droplet, $A_s(t)$, must be known before the direct contact heat-transfer rate is calculated. In the past, several investigators^{1,3,19,21} studied both

experimentally and analytically the impacting droplet dynamics. A numerical model developed by Shi and Chen¹⁹ is in good agreement with experiments, and their approximation of the instantaneous spreading diameter on a very hot surface (i.e., hotter than the Leidenfrost temperature) is adapted in this study

$$D_s(t) = 1.6 U_d^{1.1} \left[t - \frac{6.8 \sigma}{\rho_\ell D_d^3} U_d^{0.25} t^{2.95} \right] + D_d \quad (6)$$

The model predicts the spreading droplet diameter fairly well for the initial droplet diameters and impacting velocities less than 4.5 mm and 4.0 m/s, respectively. In this model, the initial deformation stage of impaction was neglected since it takes a small fraction (less than 10%) of the total spreading process. In neglecting the initial deformation stage, the initial radius of the spreading droplet upon the solid surface was taken as the initial diameter of the droplet.

In the heat-transfer analysis, however, the initial stage of droplet spreading is significant. Therefore, the spreading diameter during the initial stage of deformation was obtained by extrapolation of Eq. (6) back to the instant of impaction. Since the instantaneous value of heat transfer was given in Eq. (5), the total amount of heat transferred from a hot surface to a liquid droplet during the direct contact time can be determined by integrating over the direct contact period as the following:

$$q = \int_0^{t_c} \dot{q}(t) dt = \int_0^{t_c} q''_{s,i}(t) A_s(t) dt \quad (7)$$

Heat Transfer to Monodispersed Spray

Modeling of impacting spray heat transfer is developed through the modification of the single droplet model. If a spray impacts onto a hot surface without any interference between droplets during an impacting process, then the total heat-transfer rate from the hot surface to the droplets will be linearly proportional to the number of impacting droplets. If, however, the droplet interaction occurs, the effects of the droplet interaction must be considered in modeling of spray heat transfer. Interference between droplets of an impacting spray can be classified into two types, i.e., spreading and impacting interference as shown in Fig. 2. Spreading interference (Fig. 2a) refers to the contact between two drops upon spreading, resulting in a reduced spreading diameter. Impacting interference (Fig. 2b) refers to the contact between two drops as one drop impacts upon the other droplet while it resides on the hot surface. The effect of impacting interference on the heat transfer process was experimentally investigated by Takeuchi, et al.⁵ The heat transfer rate was found to be independent of impacting frequency, suggesting impacting interference is negligible. From their study, it was concluded that spreading interference has a much greater effect on heat transfer than impacting interference. Spreading interference directly reduces the liquid-solid contact area, while impacting interference does not significantly alter the spreading area of a droplet. Therefore, only spreading interference is considered in the present analysis. In modeling the effects of spreading interference, all the droplets distributed randomly in a conical space at an instant are assumed to lay out in a square arrangement on a square plane, as shown in Fig. 3. The bottom circular plane of the cone is transformed into a square plane. Then the dimension of the square plane, L , becomes

$$L = \sqrt{\pi} R_{sp} \quad (8)$$

In determining the number of droplets on the square plane at an instant, it is necessary to specify the time it takes for a droplet located at the exit of nozzle to travel to the heated

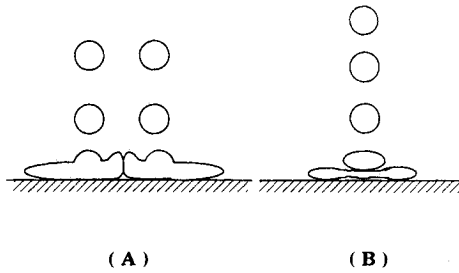


Fig. 2 Two types of droplets' interference: a) spreading interference and b) impacting interference.

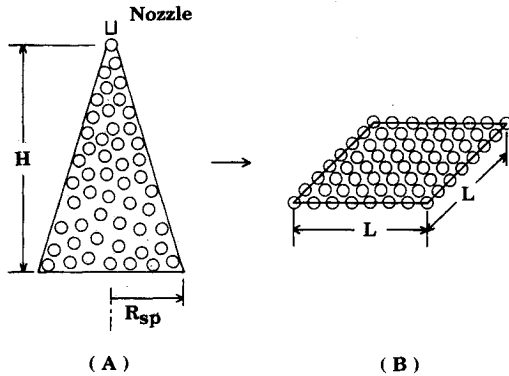


Fig. 3 Conversion of a randomly dispersed spray to a square matrix.

target. During this time interval, the number of droplets which is assumed to cross the square plane is given as

$$N = \frac{m'' A_t H}{m_d U_d} \quad (9)$$

where $A_t = \pi R_{sp}^2$.

The criterion to determine whether the spreading interference takes place or not is based on the maximum spreading diameter of a single droplet. Spreading interference occurs at a droplet number at which the distance between droplets in a square array is less than the maximum spreading diameter, hence, the droplets will contact each other upon spreading. This droplet number is termed the transition value in our analysis where the corresponding number of droplets per plane is given as

$$N_t = (L/D_{s,max})^2 \quad (10)$$

For N less than N_t , no spreading interference takes place, resulting in individual droplet impactation. However, if N is greater than N_t , spreading interference will take place. From Eq. (9), the corresponding mass flux to the transition droplet number, N_t , is given as

$$m''_t = \frac{N_t m_d U_d}{H A_t} \quad (11)$$

Once the spreading interference occurs, any impacting droplet can not fully spread to its maximum area, resulting in reduction of droplet-wall contact area. The reduction ratio of contact area due to spreading interference can be expressed as

$$i = 1 - \frac{N}{N_t} \quad (12)$$

As mass flux increases, the spreading area of individual droplets will further be reduced until total droplet spreading is completely restricted. At this point, the distance between

the droplets in a square array is equal to the initial droplet diameters, and is defined as the critical point given by

$$N_{cr} = (L/D_d)^2 \quad (13)$$

And the corresponding critical mass flux is given as

$$m''_{cr} = \frac{N_{cr} m_d U_d}{H A_t} \quad (14)$$

At this critical droplet number, the reduction ratio of contact area becomes the maximal value, i.e., $1 - N_t/N_{cr}$. As the droplet number increases beyond the critical value, N_{cr} , the reduction ratio does not increase but maintains its maximal value. The total amount of heat transferred from a hot surface to the N number of droplets during a period of impaction is calculated from Eqs. (7) through (14), and is given as follows:

$$Q = qN \quad \text{for } m'' \leq m''_t \quad (15)$$

$$Q = qN(1 - i) \quad \text{for } m''_t \leq m'' \leq m''_{cr} \quad (16)$$

and

$$Q = qN_{cr}(1 - i_{cr}) \quad \text{for } m''_{cr} \leq m'' \quad (17)$$

Eqs. (16) and (17) represent the same correlation, i.e.,

$$Q = qN_t \quad \text{for } m''_t \leq m'' \quad (18)$$

Therefore, the total energy transferred by a certain number of droplets is generally categorized into two regions according to the liquid flow rate, i.e., sparse (without droplet interaction) and dense (with droplet interaction). As mentioned before, for m'' less than m''_t no spreading interference takes place, resulting in proportional increase of heat transfer with the liquid flow rate. For m'' greater than m''_t , however, the amount of heat transfer is expected to be independent of the liquid flow rate. This postulation will be discussed further in the next section.

Results and Discussion

Single Droplet Impaction

Analytical modeling for a single isolated droplet impaction yields theoretical values of direct liquid-solid contact time, droplet spreading diameter, and total heat transfer to the droplet. The direct liquid-solid contact time is calculated from Eq. (3) at various subcooling temperatures and heater surface temperatures. Figures 4 and 5 show the effects of subcooling temperature and heater surface temperature on the contact time of a droplet of 2.3 mm diameter impacted with a velocity of 0.63 m/s. The experimental work of Inada et al.⁷ is also compared in the figures. Good agreement between the present analytical work and the experimental work is observed. Inada et al.⁷ used an optical technique, using photo detectors, to measure the transient vapor-film thickness beneath the droplet. From the traces of the vapor-film thickness, apparent duration of direct liquid-solid contact was observed. Three stages of vapor-film development were observed, i.e., direct liquid-solid contact, rapid vapor-film growth, and subsistence of a well-developed vapor film. Comparing the direct liquid-solid contact time and residence time of a droplet, it was concluded that the liquid-solid contact time could not be neglected in the calculation of single droplet impacting heat transfer. As shown in Fig. 4, the direct contact time t_c depends to a large degree upon the subcooling temperature. As subcooling increases, an extended period of direct contact is observed. This can be attributed to a longer time required for heating of the liquid before nucleate boiling occurs. The direct contact time is observed to increase with a lower heater sur-

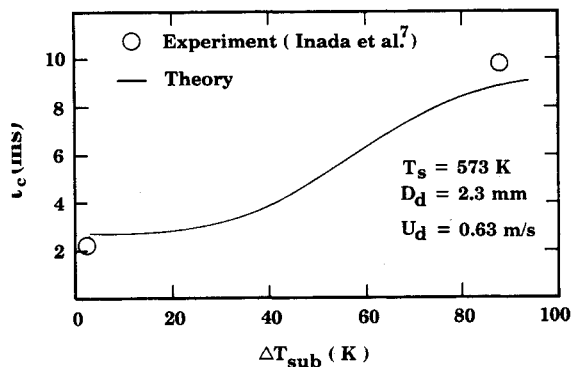


Fig. 4 Variation of direct contact time with liquid subcooling.

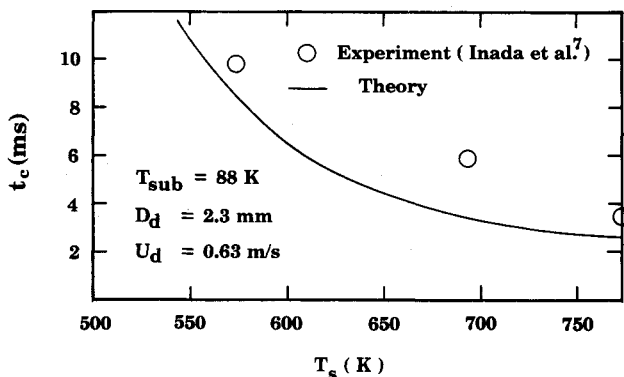


Fig. 5 Variation of direct contact time with heater surface temperature.

face temperature as shown in Fig. 5. Since the total heat-transfer rate to an impacting droplet depends to a great degree on the direct contact time and the initial wall temperature, relation of the direct contact time with the wall temperature is of great importance to the heat-transfer analysis. The effect of wall-surface temperature on the heat-transfer characteristics will be discussed later.

As shown in Eq. 3, the initial droplet size and the impacting velocity are not included in determining the direct liquid-solid contact time. However, the droplet impacting dynamics such as the droplet spreading diameter (Eq. 6) is dependent on these parameters. The impacting dynamics was usually characterized with the Weber number, We . Consequently, the direct liquid-solid contact heat transfer of single droplet depends upon both the direct contact time t_c and the impacting dynamics, as shown in Eq. (7). In order to see the effect of the Weber number on the impacting dynamics, the experimental results of Shi and Chen¹⁹ are nondimensionalized in terms of the maximum spreading diameter ratio ($D_{s,max}/D_{d,o}$) and the Weber number. These results are shown in Fig. 6. The maximum spreading diameter ratio increases monotonically with the Weber number until the Weber number reaches about 600. The total amount of heat transferred to a droplet during the direct contact time is then analytically calculated from Eq. (7). In order to eliminate the effect of the initial droplet mass, the heat-transfer value is generalized by using the heat-transfer effectiveness defined as

$$\varepsilon = \frac{q}{m_d(h_{fg} + C_p \Delta T_{sub})} \quad (19)$$

The present analytical results are nondimensionalized in terms of the Weber number and heat-transfer effectiveness, and are presented in Fig. 7. In this calculation, the liquid (water) subcooling temperature and the heater surface temperature are 84 K and 573 K, respectively. Droplet impacting velocities in the range of 0.6 to 4 m/s and droplet diameters

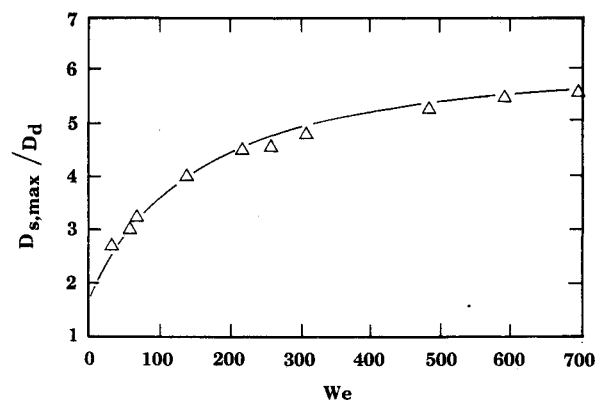
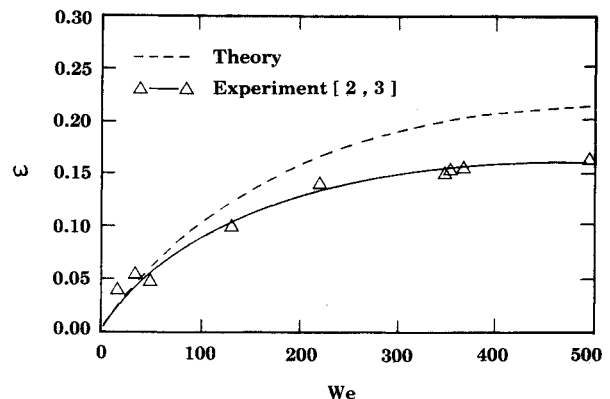
Fig. 6 Variation of maximum spreading diameter ratio ($D_{s,max}/D_d$) with the Weber number.

Fig. 7 Variation of heat transfer effectiveness with the Weber number.

in the range of 0.3 to 2.3 mm are used to vary the Weber number. To facilitate a comparison, the experimental results of Pederson² and Kendall and Rohsenow³ are rearranged in terms of the heat transfer effectiveness and the Weber number, as shown in Fig. 7. Although the analytical results predict somewhat higher effectiveness than experiments, the general trend is in good agreement. Since the heat-transfer effectiveness increases with the increased Weber number, the larger droplet has a better heat transfer capability due to increased liquid-solid contact area. As droplet size increases, the ratio of inertial forces to surface tension increases. Larger inertial forces enhance the spreading area of the impacting droplet. And since heat transfer to the droplet by conduction is dependent on direct contact area, the enlarged spreading area increases heat transfer, resulting in an increased effectiveness. When the trend of heat transfer is compared to that of maximum droplet spreading diameter, which is shown in Fig. 6, an interesting similarity between the two is observed. From this observation, it is concluded that heat transfer of a single impacting droplet depends to a great degree upon the direct liquid-solid contact behavior.

It is also interesting to observe in Fig. 7 a gradual increase of the heat-transfer effectiveness around $We = 80$, which is called the critical Weber number. It is well known that an impacting droplet in a nonwetting region tends to disintegrate if the Weber number is greater than 80 (Watchters and Westerling¹). If the impacting droplet heat transfer occurs by a mechanism other than direct contact heat transfer, such as air convective heat transfer, the resulting heat transfer should be somewhat affected by this droplet disintegration process. However, regardless of whether or not the droplets disintegrate at $We = 80$, the experimental results of heat-transfer effectiveness are observed to increase gradually with the Weber number. This observation also indicates that the direct

contact heat transfer before taking place of droplet disintegration is the most significant mechanism.

For very small droplets (i.e., diameters less than 300 μm), the present analytical model for heat transfer is not applicable due to the following two reasons: First, there is no adequate model for the droplet impaction dynamics. Presently existing models^{3,19} are not applicable for small droplets. In addition, the condition of thermodynamic equilibrium for vapor nuclei may be altered due to the increased effect of droplet surface tension as the droplet becomes small. Therefore, only droplets larger than 300 μm are considered in this study.

The effect of droplet subcooling on the heat-transfer effectiveness is compared to the experimental work of Inada et al.⁷ In Table 1, comparisons are made for an initial diameter, velocity, and heater surface temperature of 2.3 mm, 0.63 m/s, and 573 K, respectively. Droplet subcooling was varied from 2 to 84 K. As expected, effectiveness increases with increased subcooling temperature. As subcooling becomes larger, a longer period of liquid-solid contact occurs, which is due to the time required to heat the liquid before phase change takes place. Also, contributing to higher effectiveness, with a larger subcooling, the heat-transfer rate during liquid-solid contact becomes more intense.

The variation of heat transfer effectiveness with the initial wall temperature is presented in Fig. 8. The wall temperatures in the range of 523 to 723 K are investigated. Unlike the droplet subcooling effect, the wall temperature effect on the heat-transfer effectiveness is insignificant in the computed range. The reason for this is that the direct contact time decreases with the increased wall temperature, as shown in Fig. 5, while the heat flux to the droplet increases as the wall temperature increases. This phenomenon was also experimentally observed in previous literature.^{14,22} Even though monodispersed droplets were used in the experiment, when sparse sprays ($m'' < 0.025 \text{ g/cm}^2 \text{ s}$) were impacted on a hot surface at temperatures in the range of 530 to 730 K, the heat transfer rates were almost invariant with the surface temperature.

Monodispersed Spray Heat Transfer

The heat-transfer characteristics of a monodispersed spray can be classified in terms of spray mass flux into two regions: sparse and dense. In the sparse region, no interactions can occur between impacting droplets. In this low mass flux re-

gion, however, the probability of interaction between two or more droplets is very small. Therefore, evolution of spreading dynamics is taken to be identical to that of a single impacting droplet. As a result, the heat-transfer effectiveness in this sparse region is independent of mass flux and can be calculated by Eq. (19). However, at the transition point of droplet mass flux, the occurrence of droplet interactions cannot be neglected. The reduction ratio of droplet spreading area is counted in the calculation of the heat-transfer effectiveness. Therefore, in this region the heat transfer effectiveness is defined as

$$\varepsilon = \frac{Q}{m_d(h_{fg} + C_p \Delta T_{\text{sub}})N} \quad (20)$$

where Q is calculated from Eq. (18).

The heat-transfer effectiveness for the monodispersed spray is determined analytically with Eq. (19) or (20). The results are presented in Fig. 9 with comparison to the experimental results.^{5,11,22} In the low-droplet mass flux region (i.e., $m'' < 0.025 \text{ g/cm}^2 \text{ s}$), analytical results are in good agreement with the experimental data.⁵ Only a slight decrease of effectiveness was observed experimentally with increased droplet mass flux. This slight decrease is due to a small, but increasing number of droplet interactions that occur as droplet mass flux increases. Another characteristic of a sparse spray is the effect of spray parameters on heat transfer. Dependence of spray effectiveness on droplet size and impacting velocity are observed both experimentally and analytically. The effect of droplet size on the monodispersed spray ($m'' = 0.0091 \text{ g/cm}^2 \text{ s}$), where the mass flow rate was fixed, was experimentally investigated by Yao and Choi.²² They reported that the spray of large sized droplets had better heat transfer than the small sized droplets spray. This effect is due to the individual spreading dynamics of the droplets.

When the mass flux surpasses the transition point ($m''_t \approx 0.025 \text{ g/cm}^2 \text{ s}$), the droplet interaction starts to play an important role in heat transfer. The theoretical transition point is compared to the experimental finding of Yao and Choi.²² Beyond the transition mass flux, significant droplet interactions are observed to influence the heat-transfer characteristics. As shown in Fig. 9, the effectiveness decreases drastically with increased mass flux. As droplet interactions increase, the direct contact area per droplet decreases, but the mass flux increases at a greater rate, resulting in an overall decrease in effectiveness. Another interesting observation in this region is that the effect of droplet size (or Weber number) on the heat transfer characteristics becomes less significant. This observation was also presented in the experimental work of Choi and Yao.¹⁴ In the transition region, however, theory predicts a more rapid decrease than does the experimental result. The present analysis seems to predict an exaggerated effect of interference on the droplet contact area and heat transfer.

Table 1 Effect of liquid subcooling on heat transfer

$\Delta T_{\text{sub}}, \text{ K}$	ε	
	Theory	Experiment (Inada et al. ⁷)
2	0.023	0.04
30	0.065	0.09
84	0.18	0.27

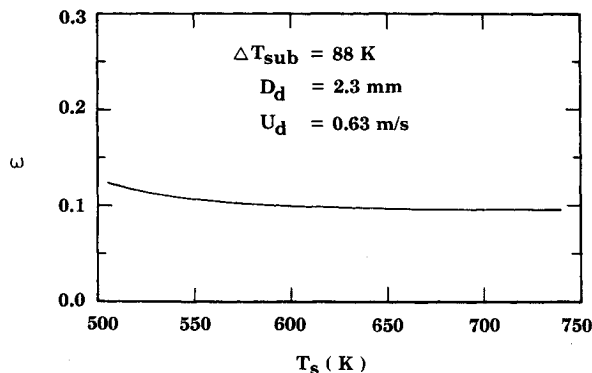


Fig. 8 The heat-transfer effectiveness profile with heater surface temperature.

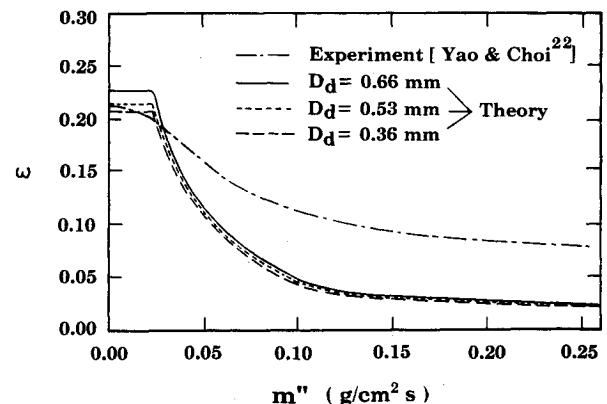


Fig. 9 Variation of heat-transfer effectiveness with spray mass flux.

This disagreement can be attributed to the geometric simplification of a randomly dispersed spray as a square arrangement of droplets on a square plane, as shown in Fig. 3b. In the square arrangement, it is assumed that the droplet spreading process is interfered with four adjacent droplets at four points 90 deg apart. With spreading interference, the shortened process ends with the droplet being symmetrically restrained to a disk shape by adjacent droplets. In contrast, in a randomly dispersed spray the spreading droplet will be restrained unsymmetrically in only one or two directions. In the unrestricted directions, spreading may be unaffected or even enhanced, as the spreading droplet may be altered from its spreading disk shape. In the real case, the spreading contact area would be larger than that modeled by the square matrix model, contributing to a higher heat-transfer effectiveness. Moreover, in the randomly dispersed actual spray, interfering droplets will be impacting at various times and, therefore, interfering during different stages of impaction. These differences between the square matrix model and a randomly distributed spray contribute to the difference in the effectiveness.

As the droplet mass flux increases, the spreading of individual droplets is further restricted until the droplet mass flux increases to the critical value m''_{cr} , where little droplet spreading is possible. Both theory and experiment indicate that the critical value is observed at about $0.1 \text{ g/cm}^2 \text{ s}$. Beyond this point the heat-transfer rate to the spray is assumed to be constant due to the complete restriction of droplet spreading. Therefore, in this region, the heat-transfer effectiveness varies inversely with the mass flux. Another observation from the present analysis is that the heat-transfer effectiveness is little affected by the droplet size in the dense flow rate region. This is due to the complete restriction of droplet spreading. Consequently, the overall droplet impacting dynamics is insignificant to the heat-transfer behavior of dense sprays. The observation was verified by Hoogendoorn and den Hond's experiments.²³ They reported that droplet size in the tested range from 0.2–1 mm and impacting velocity in the range of 10–30 m/s had little effect on the cooling by dense sprays, rather than the overall mass flux being most important. The analytical work, however, predicts much lower effectiveness than the experimental work of Yao and Choi²² and Bolle and Moureau,⁸ as shown in Fig. 9. This discrepancy has two contributing factors; theoretical calculations do not account for secondary droplet impactions and are based on the assumption that total heat flux remains constant in the dense spray region. In the experimental work, sprays were impacted vertically onto a horizontal surface. In this orientation, droplets may impact upon the surface more than once, increasing the heat transfer to the spray. Since the present theory does not take into account secondary impactions, it predicts a lower effectiveness. The effect of secondary droplet impactions upon heat transfer was studied by Choi and Yao,¹⁴ and found to increase heat transfer by 1.5 times. This explains a large portion of the discrepancy between theory and experiment, but even with this effect the experimental effectiveness is still high. Some discrepancy may be attributed to assuming that heat transfer does not increase in the dense region of liquid spray. In fact, the heat transfer was observed to increase with increased mass flux to a certain degree.

Conclusion

From the present analysis of direct liquid-solid contact heat transfer of monodispersed droplets impacting onto a hot surface, the following conclusions are drawn:

- 1) Droplet-wall interaction can be described as a two-step process; a period of direct contact between spreading droplet and hot surface, followed by formation of a well-developed vapor film.
- 2) Conduction to the droplet during the direct liquid-solid contact time is the dominant mode of droplet impacting heat transfer.

3) The effect of liquid subcooling on the heat-transfer effectiveness is very significant, while the solid surface temperature is less significant in the tested temperature range.

4) Interaction between the droplets in a randomly dispersed spray is modeled by approximating the conical spray pattern as a square matrix of drops. Based on the square matrix model, a spray can be classified as sparse or dense. The mass flux at which droplet interactions become significant is $0.025 \text{ g/cm}^2 \text{ s}$.

5) In the sparse region (i.e., $m'' < 0.025 \text{ g/cm}^2 \text{ s}$), droplet impacting dynamics were found to have a significant effect on the heat-transfer effectiveness. The effectiveness is found to increase with increased Weber number. In the dense region (i.e., $m'' > 0.025 \text{ g/cm}^2 \text{ s}$), the effect of droplet impacting dynamics becomes insignificant, but the overall mass flux is the most important to the total heat-transfer rate.

6) In evaluating the usefulness of the square matrix model used in this study, it can be said that it reasonably well predicts the criterion at which droplet interactions begin to affect the heat-transfer characteristics. Possible improvement of droplet interaction modeling would be done by considering matrix configurations other than a square or perhaps a parabolic model based on a Gaussian distribution.

Acknowledgment

Support for this work from the National Science Foundation (CBT-8708705) is gratefully appreciated.

References

- ¹Wachters, L. H. J., and Westerling, N. A. J., "The Heat Transfer from a Hot Wall to Impinging Water Drops in the Spheroidal State," *Chemical Engineering Science*, Vol. 21, 1966, pp. 1047–1056.
- ²Pederson, C. O., "An Experimental Study of the Dynamic Behavior and Heat Transfer Characteristics of Water Droplets Impinging Upon a Heated Surface," *International Journal Heat Mass Transfer*, Vol. 13, 1970, pp. 369–381.
- ³Kendall, G. E., and Rohsenow, W. M., "Heat Transfer to Impinging Drops and Post Critical Heat Flux Dispersed Flow," Report of Heat Transfer Laboratory, Massachusetts Institute of Technology, No. 85694-100, 1978.
- ⁴Shoji, M., Wakunaga, T., and Kodama, K., "Heat Transfer from a Heated Surface to an Impinging Subcooled Droplet (Heat Transfer Characteristics in the Non-Wetting Regime)," *Heat Transfer Japanese Research*, Vol. 13, No. 3, 1984, pp. 50–67.
- ⁵Takeuchi, K., Senda, J., and Yamada, K., "Heat Transfer Characteristics and the Break-Up Behavior of Small Droplets Impinging Upon a Hot Surface," ASME-JSME Thermal Engineering Joint Conference, Honolulu, Hawaii, Vol. 1, 1983.
- ⁶Styrikovich, M. A., Lamden, D. I., and Kostanovskaya, M. E., "Space-Time Structure of Thermal Interaction in the Brief Contact of a Liquid Droplet with a Supercritically Heated Surface," *High Temperature*, Vol. 24, No. 4, 1986, pp. 577–585.
- ⁷Inada, S., Miyasaka, Y., Sakamoto, K., and Hojo K., "Liquid-Solid Contact State and Fluctuation of the Vapor Film Thickness of a Drop Impinging on a Heated Surface," *Journal of Chemical Engineering of Japan*, Vol. 21, No. 5, 1988, pp. 463–468.
- ⁸Inada, S., Miyasaka, Y., and Nishida, "Transient Heat Transfer for a Water Drop Impinging on a Heated Surface," *Bulletin JSME*, Vol. 28, No. 246, 1985, pp. 2675–2681.
- ⁹Mizikar, E., "Spray Cooling Investigation for Continuous Casting of Billets and Blooms," *Iron and Steel Engineering*, Vol. 47, June, 1970, pp. 53–70.
- ¹⁰Hall, P. C., "The Cooling of Hot Surfaces by Water Sprays," Central Electricity Generating Board, RD/B/N3361, 1975.
- ¹¹Bolle, L., and Moureau, J. C., "Experimental Study of Heat Transfer by Spray Cooling: Heat and Mass Transfer in Metallurgical Systems," Hemisphere Publishing Corp., Washington, DC, pp. 527–534.
- ¹²Liu, L., and Yao, S. C., "Heat Transfer Analysis of Droplet Flow Impinging on a Hot Surface," *Proceeding of the 7th Int. Heat Transfer Conference*, Vol. 4, 1982, pp. 161–166.
- ¹³Toda, S., "A Study of Mist Cooling (2nd Report: Theory of Mist Cooling and Its Fundamental Experiments)," *Heat Transfer Japanese Research*, Vol. 1, No. 3, 1972, pp. 39–50.

¹⁴Choi, K. J., and Yao, S. C., "Mechanisms of Film Boiling Heat Transfer of Normally Impinging Spray," *International Journal Heat Mass Transfer*, Vol. 30, No. 2, pp. 311-318, 1987.

¹⁵Hsu, Y. Y., "On the Size Range of Active Nucleation Cavities on a Heating Surface," *Journal of Heat Transfer*, Vol. 84, Aug., 1962, pp. 207-216.

¹⁶Han, C., and Griffith, P., "The Mechanism of Heat Transfer in Nucleate Pool Boiling—Part I," *International Journal Heat Mass Transfer*, Vol. 8, 1965, pp. 887-904.

¹⁷Brown, W. T., "A Study of Flow Surface Boiling," Ph.D. dissertation, Massachusetts Institute of Technology, Mech. Eng. Dept. (1967).

¹⁸Carslaw, H. S., and Jaeger, J. C., "Conduction of Heat in Solids," 2nd ed. Oxford University Press, Oxford, 1959, p. 88.

¹⁹Shi, M. H., and Chen, J. C., "Behavior of a Liquid Droplet Impinging on a Solid Surface," ASME 83-WA/HT-104.

²⁰Inada, S., Miyasaka, Y., Nishida, K., and Chandratilleke, G. R., "Transient Temperature Variation of a Hot Wall Due to an Impinging Drop-Effect of Subcooling of the Water Drop," ASME-JSME Thermal Engineering Joint Conference, Vol. 1, 1983, pp. 173-182.

²¹Ueda, T., Enomoto, T., and Kanetsuki, M., "Heat Transfer Characteristics and Dynamic Behavior of Saturated Droplets Impinging on a Heated Vertical Surface," *Bulletin JSME*, Vol. 22, No. 167, 1979, pp. 724-732.

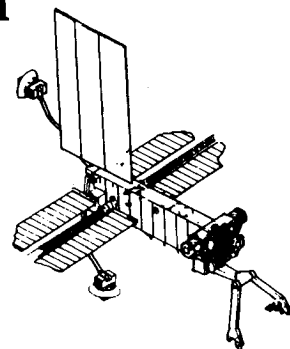
²²Yao, S. C., and Choi, K. J., "Heat Transfer Experiments of Mono-Dispersed Vertically Impacted Sprays," *International Journal Multiphase Flow*, Vol. 13, No. 5, 1978, pp. 639-648.

²³Hoogendoorn, C. J., and den Hond, R., "Leidenfrost Temperature and Heat Transfer Coefficients for Water Sprays Impinging on a Hot Surface," *Proceeding of the Fifth International Heat Transfer Conference*, Vol. 4, 1974, pp. 135-138.



Space Stations and Space Platforms—Concepts, Design, Infrastructure, and Uses

Ivan Bekey and Daniel Herman, editors



This book outlines the history of the quest for a permanent habitat in space; describes present thinking of the relationship between the Space Stations, space platforms, and the overall space program; and treats a number of resultant possibilities about the future of the space program. It covers design concepts as a means of stimulating innovative thinking about space stations and their utilization on the part of scientists, engineers, and students.

To Order, Write, Phone, or FAX:



American Institute of Aeronautics and Astronautics
c/o TASCOT
9 Jay Gould Ct., P.O. Box 753, Waldorf, MD 20604
Phone (301) 645-5643 Dept. 415 FAX (301) 843-0159

1986 392 pp., illus. Hardback
ISBN 0-930403-01-0 Nonmembers \$69.95
Order Number: V-99 AIAA Members \$43.95

Postage and handling fee \$4.50. Sales tax: CA residents add 7%, DC residents add 6%. Orders under \$50 must be prepaid. Foreign orders must be prepaid. Please allow 4-6 weeks for delivery. Prices are subject to change without notice.